Estimating Rolling Element Bearing Stiffness Under Different Operational Conditions Through Modal Analysis

William Jacobs, Rene Boonen, Paul Sas and David Moens

Abstract This paper presents a novel test rig, developed to analyse the behaviour of rolling element bearings subjected to highly varying loads. The design is optimised to measure the bearing behaviour, free from dynamics of the surrounding structure. In the current study, the test rig is used to evaluate the stiffness of a deep groove ball bearing under different operational conditions. The bearing behaviour is measured using the modal analysis technique. Then, an analytical model of the test structure is fitted on the data to estimate the bearing stiffness. The stiffness estimation is validated using a dummy bearing with a known stiffness. Finally, the stiffness of a mounted ball bearing is estimated. The paper evaluates the effect of a radial static load on the bearing stiffness. Stationary and operational conditions are compared as well. A clear difference between the stiffness of a rotating and non-rotating bearing is observed.

Keywords Rolling element bearing stiffness · Modal analysis

1 Introduction

In open literature, little information on the characteristics of rolling element bearings under dynamic conditions is available. This is probably due to the difficulty of performing a sufficiently accurate measurement and the multitude of

W. Jacobs (✉) · R. Boonen · P. Sas
Department of Mechanical Engineering, KU Leuven,
Celestijnenlaan 300B, 3001 Heverlee, Belgium
e-mail: william.jacobs@mech.kuleuven.be

D. Moens
Campus De Nayer, Department of Applied Engineering, Lessius Mechelen,
Jan De Nayerlaan 5, 2860 Sint-Katelijne-Waver, Belgium
e-mail: david.moens@mech.kuleuven.be

D. Moens
Department of Mechanical Engineering, KU Leuven, Leuven, Belgium

G. Dalpiaz et al. (eds.), *Advances in Condition Monitoring of Machinery in Non-Stationary Operations*, Lecture Notes in Mechanical Engineering,
DOI: 10.1007/978-3-642-39348-8_8,

parameters influencing the results [1]. Some information is available on the dynamics of machine tool spindles, as part of research conducted in the seventies. An overview is given in [2]. Special rigs were built for excitation and response measurement of the rotor. It was concluded that the dynamics of the bearings are mainly influenced by their preload, speed, lubricant and clearance.

Recently, a novel rolling element bearing test rig was developed at KU Leuven. The test rig is able to apply a fully controlled multi-axial static and dynamic load on the bearing. Also, different types and sizes of bearings can be mounted. As the load acting on the bearing is well-known, load identification techniques can be developed and validated. Furthermore, the influence of dynamic excitations on the lifetime of bearings can be investigated. Finally, bearing models can be validated using this test rig. In the current study, the relation between an external dynamic load and the bearing response is analysed. Also, the bearing stiffness is experimentally determined for different load and speed conditions.

This paper first introduces the test rig in Sect. 2. A full review of the test rig can be found in an earlier publication of the authors [3]. In order to understand the bearing response, the dynamics of the surrounding structure should be known. Sect. 3 of the paper therefore details about the test rig dynamics. In Sect. 4, an analytical model to estimate the bearing stiffness from modal measurements is introduced. The stiffness measurement is experimentally validated in Sect. 5, using a dummy bearing with a known stiffness. In the last section, the stiffness of a deep groove ball bearing is analysed for different operational conditions.

2 Test Rig Design

The main concept of the test rig is outlined in Fig. 1. An electric motor drives a shaft through a flexible coupling. The shaft is supported by two bearings, forming a rigid spindle. At the end of the shaft, a third bearing is mounted. This is the test bearing. The load is directly applied on the stationary outer ring of the test bearing.

The rig makes it possible to test bearings of different types, such as deep groove ball bearings and tapered roller bearings, and bearings of different sizes. Using a clamping mechanism called collet chuck, the shaft can be adjusted to fit different bearings. The test bearing is mounted on a small auxiliary shaft, adapted to its bore

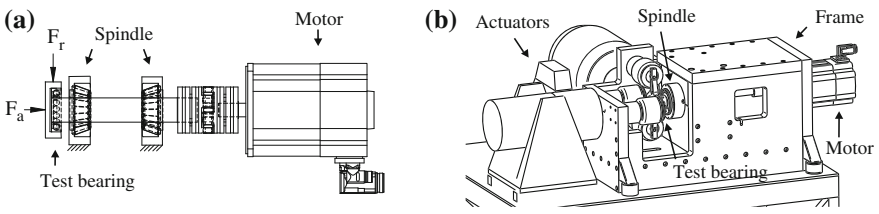

Fig. 1 Concept **a** and overview **b** of the test rig

diameter. After inserting this auxiliary shaft into the main shaft of the spindle, the locknut is tightened forming a stiff connection between both shafts. Also, using an intermediate adaptor sleeve in between the bearing and the housing, different bearings can be fitted in the housing.

The load imposed on the bearing is controlled in the radial and axial direction, independent of each other. Furthermore, the load has a static and dynamic component in both directions. In this way, it is possible to simulate different real-life situations, where i.e. gear meshing forces are acting on the bearing. Air springs apply a static force up to 10 kN, while electrodynamic shakers generate a dynamic force with an amplitude up to 1 kN and a frequency up to 500 Hz, in each direction. Figure 2 gives an overview of the actuator configuration. The static load is generated by four air springs, transferring their force to the bearing using an arm on the housing. Two air springs control the axial force ($F_{a,st}$) and two air springs control the radial force ($F_{r,st}$). The dynamic load is directly introduced on the bearing housing through the stingers of the shakers: one stinger for the axial direction ($F_{a,d}$) and one stinger for the radial direction ($F_{r,d}$).

3 Test Rig Dynamics

In order to enable a correct interpretation of the bearing measurements, the dynamics of the test rig should be analysed first. Both the housing of the test bearing and the frame of the test rig are solid structures, designed to keep the resonances of the rig outside the range of the bearing excitation up to 500 Hz. According to finite element (FE) calculations, the first flexible mode of the assembly housing and sleeve occurs at a resonance frequency of 695 Hz. The frame shows a first flexible mode at 663 Hz. It is a closed and rigid structure, mounted on four bushings. The bushings dynamically decouple the frame from the

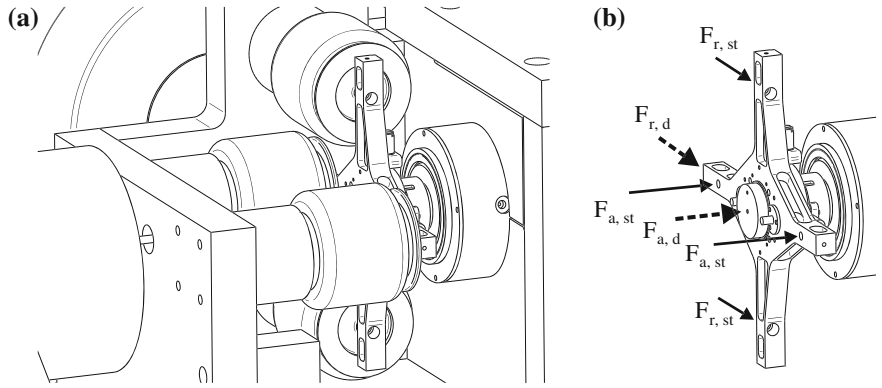

Fig. 2 Actuators **a** and their corresponding force vectors **b**

environment. The six rigid body modes of the test rig moving on its bushings are all located between 4 and 16.4 Hz. An earlier publication of the authors [4] details about the dynamics of the bearing housing and the frame, including modal analyses to validate the FE calculations.

The spindle of the test rig consists of a solid shaft, supported by two tapered roller bearings in a cylindrical housing. The tapered roller bearings are mounted in O-configuration and axially preloaded to increase the bending stiffness of the spindle. During design, a one-dimensional model of the stepped shaft is used to evaluate its dynamics. The stiffness of the bearings depends on the axial preload, and is estimated based on [6]. A radial stiffness of 510×10^6 N/m, an axial stiffness of 263×10^6 N/m and a tilt stiffness of 160×10^3 Nm/rad is used. The shaft is connected to the motor through a flexible coupling, decoupling both parts dynamically. Only the mass of the vibrating part of the coupling should be taken into account. It is modeled as a point mass. The test bearing housing is modeled as a point mass as well, as its dynamics were analysed separately. In between the bearing housing and spindle shaft, a stiffness element is added. It represents the test bearing. The value of this stiffness is set to 35×10^6 N/m, an average value of the possible test bearing stiffness's. The FE model and the first five modes are shown in Fig. 3. The third mode, at 1,012 Hz, is the rigid body mode of the shaft in which the shaft axially translates.

In order to understand the test bearing movement, the frequency response function (FRF) between an input force on the bearing housing and the displacement of the test bearing is analysed. Figure 4 shows the displacement of the housing mass (*solid line*) and the displacement of the bearing seat on the front of the shaft (*dashed line*). At 530 Hz, a strong displacement of the housing mass moving on the test bearing stiffness is observed. This resonance corresponds to the second mode of Fig. 3. It is not a spindle mode, as it only appears due to the connection with the test bearing and the housing mass. The other modes of Fig. 3

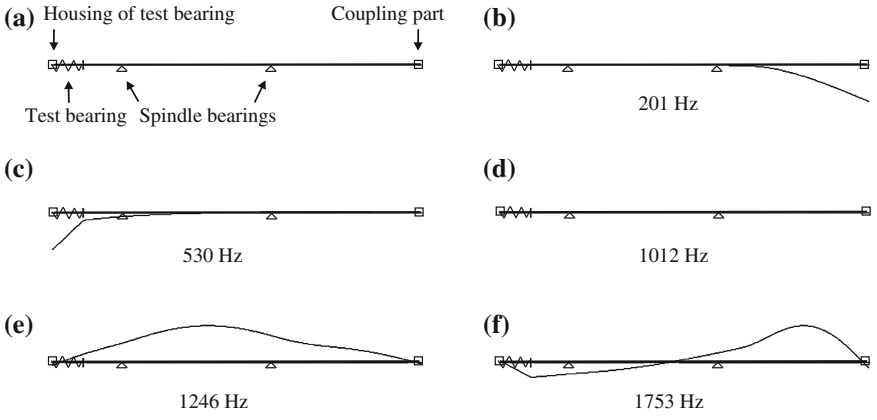

Fig. 3 Model **a** and first five modes **b–f** of the spindle and test bearing assembly

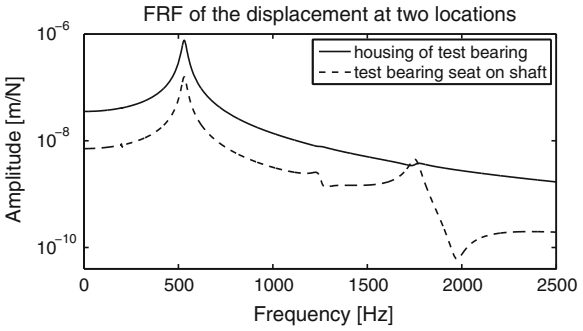

Fig. 4 FRF of the displacement at two locations of the FE model

are spindle modes. Clear radial motion of the test bearing seat on the shaft first appears at 1,753 Hz. Also recalling the third mode of Fig. 3, axial motion of the test bearing seat first appears at 1,012 Hz. Therefore, it is concluded that the bearing can be excited up to 500 Hz, without any influence of the spindle dynamics.

To validate the spindle dynamics, the modes of the shaft were experimentally measured. A shaker load is introduced on the test bearing housing, while 3 accelerometers measure the response of the shaft. As the spindle shaft is mounted in a cylindrical housing, it was only possible to install accelerometers on the front and the back of the shaft. Therefore, a full modal analysis could not be performed. Figure 5 shows the sum of FRFs of the 3 accelerometer signals. To analyse the effect of the air spring load on the spindle dynamics, the measurement was repeated for different load levels of the air springs. The FRFs are highly influenced by structural resonances of the different test rig components above 700 Hz. Also, below 150 Hz, tilt modes of the test bearing influence the FRFs. Nevertheless, the first and fifth spindle mode of the simulation, having a high response at the sensor locations, could be identified. The first mode appears at 287 Hz. The fifth mode was found at 1,899 Hz for 500 N radial load, 1,908 Hz for 1,000 N radial load and 1,915 Hz for 1,500 N radial load. As the radial load acting on the tapered roller bearings, introduced by the air springs, is very small compared to the axial preload, the stiffness of the spindle is only little affected by the air pressure. The location of this fifth mode is used in the next section to improve the estimation of the test bearing stiffness.

4 Analytic Model to Estimate the Bearing Stiffness

The FE model of the previous section shows a clear rigid body motion of the test bearing housing moving on the bearing stiffness. The frequency of this rigid body mode is mainly determined by the stiffness of the test bearing. Therefore, identification of the mode is used to estimate the bearing stiffness. In the current study,

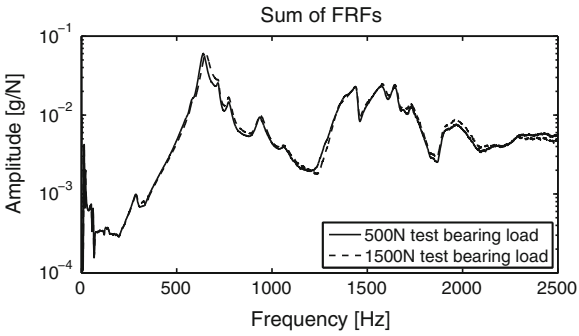

Fig. 5 Sum of FRFs of modal analysis spindle

a deep groove ball bearing 6302 is mounted. Five accelerometers are used to measure the motion of the test bearing housing. A full review of this measurement is given in [4]. In order to estimate the bearing stiffness, a model is fitted on the measured FRFs. For example an analytical model or a multi-body model can be used. Here, the radial bearing vibrations is described by the analytical model of Fig. 6. The parameters of the model are summarized in Table 1.

Each mass has one degree of freedom, namely a displacement in the vertical direction. Also, a vertical force acts on m_H, representing the shaker force. Since the housing of the test bearing has its first flexible mode at 695 Hz, it is considered as a single mass below this frequency. The value of this mass m_H is known from CAD. The spindle is represented by a single spring k_S and mass m_S. This is valid for excitations up to 1,908 Hz. Above this frequency, flexible modes of the spindle influence the results. The frame is considered as a single mass m_F for excitations up to 660 Hz, its first flexible mode. Both k_B and k_{AS} are derived from data provided by the manufacturer of the bushings and air springs. In order to determine the values of the combined stiffness k_{TB+MS}, the bending stiffness k_S and the masses m_S and m_F, the model is fitted on measured FRFs. The stiffness k_{TB+MS} is the combination of k_{TB} and k_{MS} in series. The bending stiffness k_S is considered constant for different test bearing loads, as the measured bending mode of the spindle is only little affected by this load. The masses m_S and m_F are the equivalent

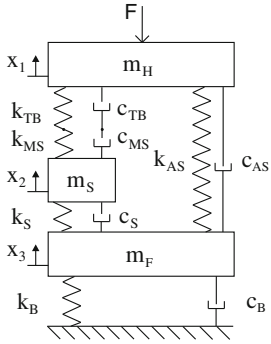

Fig. 6 Analytic model to estimate the bearing stiffness

Table 1 Parameters of the 3DOF model

Parameter	Description	Value
m_H	Mass of the test bearing housing	2.566 kg
m_S	Equivalent mass of the spindle	2.8 kg
m_F	Equivalent mass of the frame	205 kg
k_{TB}	Stiffness of the test bearing	To be determined
k_{MS}	Stiffness of the mounting system	114×10^6 N/m
k_{AS}	Combined stiffness of the air springs	650×10^3 N/m
k_S	Bending stiffness of the spindle	348×10^6 N/m
k_B	Combined stiffness of the bushings	180×10^3 N/m

masses of both the spindle and the frame, concentrated at the location of the test bearing. The simulated system has three natural frequencies, tuned according to their value as experimentally measured:

- 4.7 Hz: the motion of m_F moving on the bushing stiffness k_B.
- 626 Hz: the motion of m_H moving on the stiffness k_{TB+MS}.
- 1,908 Hz: the first bending mode of the spindle shaft exciting the bearing.

The stiffness of the modular mounting system of the test bearing, as described in Sect. 2, is combined into k_{MS}. It comprises the stiffness of the bearing housing, the intermediate sleeve, the auxiliary shaft and the collet chuck. All the connections, the line contact between the housing and the sleeve, the sleeve and the bearing, the bearing and the shaft and the chuck connection between the auxiliary shaft and spindle shaft are included as well. The stiffness k_{MS} is measured experimentally using a solid bearing, a steel disk with the same dimensions as the test bearing. Since the stiffness of the steel disk is at least a factor 10 higher than k_{MS}, k_{TB+MS} approximates k_{MS}. Therefore, k_{MS} is identified using the same modal analysis as applied to determine the test bearing stiffness, now with the steel disk mounted in the test rig and neglecting k_{TB} in the model.

Figure 7 compares the measured *(black lines)* and calculated *(grey lines)* FRFs when the test bearing is inserted. Below 150 Hz, the measured FRFs are influenced by the tilt modes of the bearing, which are not modeled. Above 700 Hz, the flexible modes of the surrounding structure appear. However, in between 150 and 700 Hz, the correspondence between the model and the measurements is good. It can be noted that the axial translational mode of the bearing influences the measurement around 300 Hz, an effect which is not observed in the simulated FRFs.

5 Validation of the Stiffness Estimation

To validate the stiffness estimation, a dummy bearing with a known stiffness is mounted in the test rig. The design of the dummy bearing is shown in Fig. 8a. It consists of an inner ring, outer ring, and a flexible structure in between.

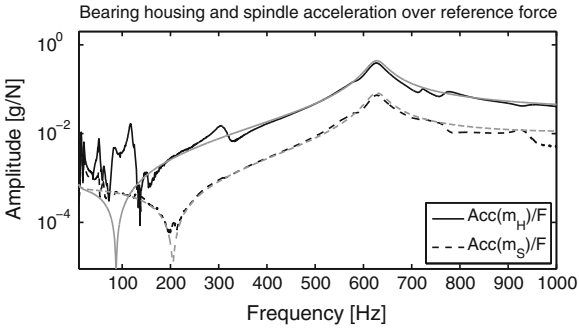

Fig. 7 Comparison between measurements and 3DOF model

The intermediate structure contains 4 leaf springs, resulting in a stiffness comparable to a normal test bearing stiffness. The stiffness is mainly determined by the thickness of the leaf springs, and accurately defined using the 2D FE model of Fig. 8b. The dummy bearing was manufactured through electric discharge machining (EDM) of a Sverker steel disk, obtaining a precision on its dimension of 0.02 mm. To take into account the variability on the geometry and the material properties, the stiffness was determined for two different models:

- Model 1: the thicknesses of the leaf springs are 0.02 mm smaller than their nominal values, the Young's modulus of the material is 200 GPa. This model serves as a lower bound for the actual stiffness, the calculated stiffness is 31.14×10^6 N/m.
- Model 2: the thicknesses of the leaf springs are 0.02 mm bigger than their nominal values, the Young's modulus of the material is 210 GPa. This model serves as an upper bound for the actual stiffness, the calculated stiffness is 34.12×10^6 N/m.

The stiffness of the dummy bearing is measured at different load levels of the air springs. The measurement is repeated to check the repeatability. The results are given in Fig. 9. The stiffness increases slightly as the load level increases. This, most likely due to an increase of stiffness in the line contacts of the mounting system, an effect which is not incorporated in k_{MS}. The grey areas indicate the

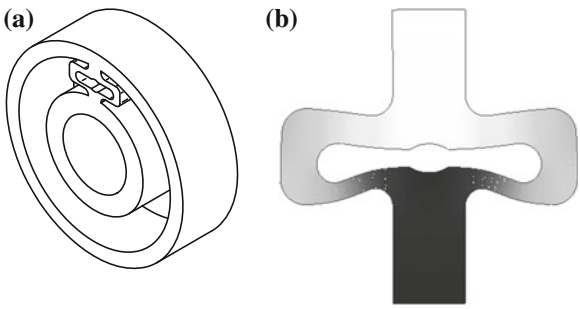

Fig. 8 Design **a** and deformation **b** of dummy bearing

upper and lower limit of the stiffness, given by the FE model. In conclusion, the estimated stiffness is within the limits of the model. Also, the repeatability of the estimation is good.

6 Bearing Stiffness Under Different Operational Conditions

In this final section of the paper, the measurements of the dynamic bearing response are combined with the 3DOF model to estimate the bearing stiffness of the mounted test bearing in different operational conditions. The influence of the radial static load on the bearing is analysed. Also, the influence of the bearing speed is investigated.

As the radial static load on a bearing increases, the stiffness of the bearing in the direction of the static load increases. More rolling elements transfer the load through the bearing and the contact surface between the rolling elements and the rings increases. Also, the stiffness of all the line contacts in the system increases. Table 2 summarizes the estimated bearing stiffness k_{TB} for different radial loads.

Next, the influence of the bearing speed is analysed. Tests at the same and different speeds are performed, and the bearing stiffness k_{TB} is estimated. The results are summarized in Table 3. It is concluded that the speed has no significant influence on the stiffness. This conclusion corresponds to the observations of [1, 5]. The spread on the stiffness estimation at different speeds is very small, and equal to the spread on the estimation at the same speeds.

Finally, the bearing stiffness of a non-rotating bearing is estimated. Table 4 shows the stiffness for three different positions of the shaft. When changing the position of the shaft, the configuration of the rolling elements in the loaded zone of the bearing changes. Therefore, a slight change in stiffness can be expected. More importantly, the stiffness of the rotating bearing is significantly lower than the stiffness of the non-rotating bearing. A mean decrease of 8.8 % is noted when the bearing is put in operation. Future research will analyse the effect on the bearing

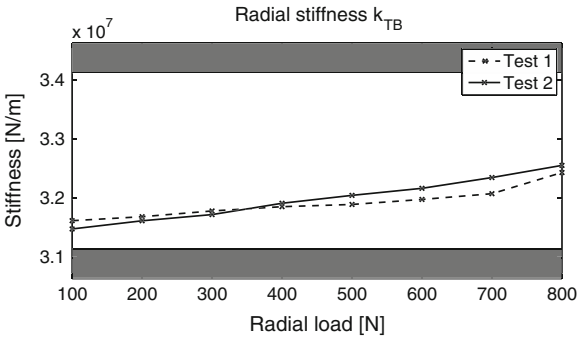

Fig. 9 Measured radial stiffness of the dummy bearing

Table 2 Influence of radial load on bearing stiffness (at 600 RPM)

Load (N)	Resonance (Hz)	Stiffness (N/m)
500	551.7	46.1×10^6
1,000	570.1	51.3×10^6
1,500	586.9	56.6×10^6

Table 3 Influence of speed on bearing stiffness (at 1,000 N radial load)

Speed (RPM)	Resonance (Hz)	Stiffness (N/m)
600	572.9	52.1×10^6
600	570.1	51.3×10^6
1,200	570.6	51.4×10^6
1,200	572.1	51.9×10^6

Table 4 Influence of shaft position on bearing stiffness (at 0 RPM and 1,000 N radial load)

Position	Resonance (Hz)	Stiffness (N/m)
1	583.5	55.5×10^6
2	586.4	56.4×10^6
3	588.0	57.0×10^6

stiffness of both the increased temperature and the formation of the lubricant film, when the bearing is put in rotation.

7 Conclusion

An innovative and versatile bearing test rig has been developed. The test rig allows easy adjustment to mount different types and sizes of rolling element bearings. The bearings can be preloaded up to 10 kN, and excited up to 500 Hz. In this way, a wide range of bearings can be tested in real-life conditions. The test rig is developed to analyse the behaviour of rolling element bearings subjected to highly varying loads. The paper shows that the design is optimised to measure the bearing behaviour, free from dynamics of the surrounding structure.

In the current study, the test rig is used to evaluate the stiffness of a deep groove ball bearing under different operational conditions. To estimate the stiffness, an analytical model of the test rig is introduced. The stiffness estimation is then validated using a dummy bearing with a known stiffness. It is shown that the stiffness of the bearing can be accurately measured. Finally, the paper evaluates the effect of a radial static load on the estimated bearing stiffness. Stationary and operational conditions are compared as well. A clear difference between the stiffness of a rotating and non-rotating bearing is observed. Future research will aim to explain this difference.

Acknowledgments This research is funded by a Ph.D. grant of the Agency for Innovation by Science and Technology (IWT). Part of this work was performed through the support of the IWT SBO-project Prognostics for Optimal Maintenance.

References

1. Kraus J, Blech J, Braun S (1987) In situ determination of rolling bearing stiffness and damping by modal analysis. J Vib Acoust Stress Reliab Design 109:235
2. Stone B (1982) The state of the art in the measurement of the stiffness and damping of rolling element bearings. CIRP Annals-Manuf Technol 31(2):529–538
3. Jacobs W, Boonen R, Sas P, Moens D (2012) The effect of external dynamic loads on the lifetime of rolling element bearings: accurate measurement of the bearing behaviour. J Phys: Conf Series 364(1):
4. Jacobs W, Boonen R, Sas P, Moens D (2012) Measuring the rigid body behaviour of a deep groove ball bearing setup. Proceedings of ISMA2012-USD2012, pp 715–726
5. Guo Y, Parker R (2012) Stiffness matrix calculation of rolling element bearings using a finite element/contact mechanics model. Mechanism and Machine Theory, pp 32–45
6. Brändlein J, Eschmann P, Hasbargen L, Weigand K (1999) Ball and Roller Bearings: Theory, Design and Application, Wiley, UK